3.2.2 Cloud phase function

We further investigate how assumptions in cloud phase function affect the spectrally-invariant behavior, by replacing the Henyey-Greenstein to a Mie phase function. Figure 7 shows for band B1, the difference in slopes and intercepts from these phase functions is negligible. For band B5, the slope and intercept are more sensitive to phase function at 4 μm than those at 8 μm. Compared to results using Henyey-Greenstein phase function, Figure 7c shows that the difference in slopes between 4 and 8 μm is less notable using the Mie phase function. Similarly, Fig. 7d shows the difference in intercepts between 4 and 8 μm is also less pronounced using the Mie phase function than that using the Henyey-Greenstein phase functions. This implies that for retrieval purpose, the use of a more accurate phase function is necessary.

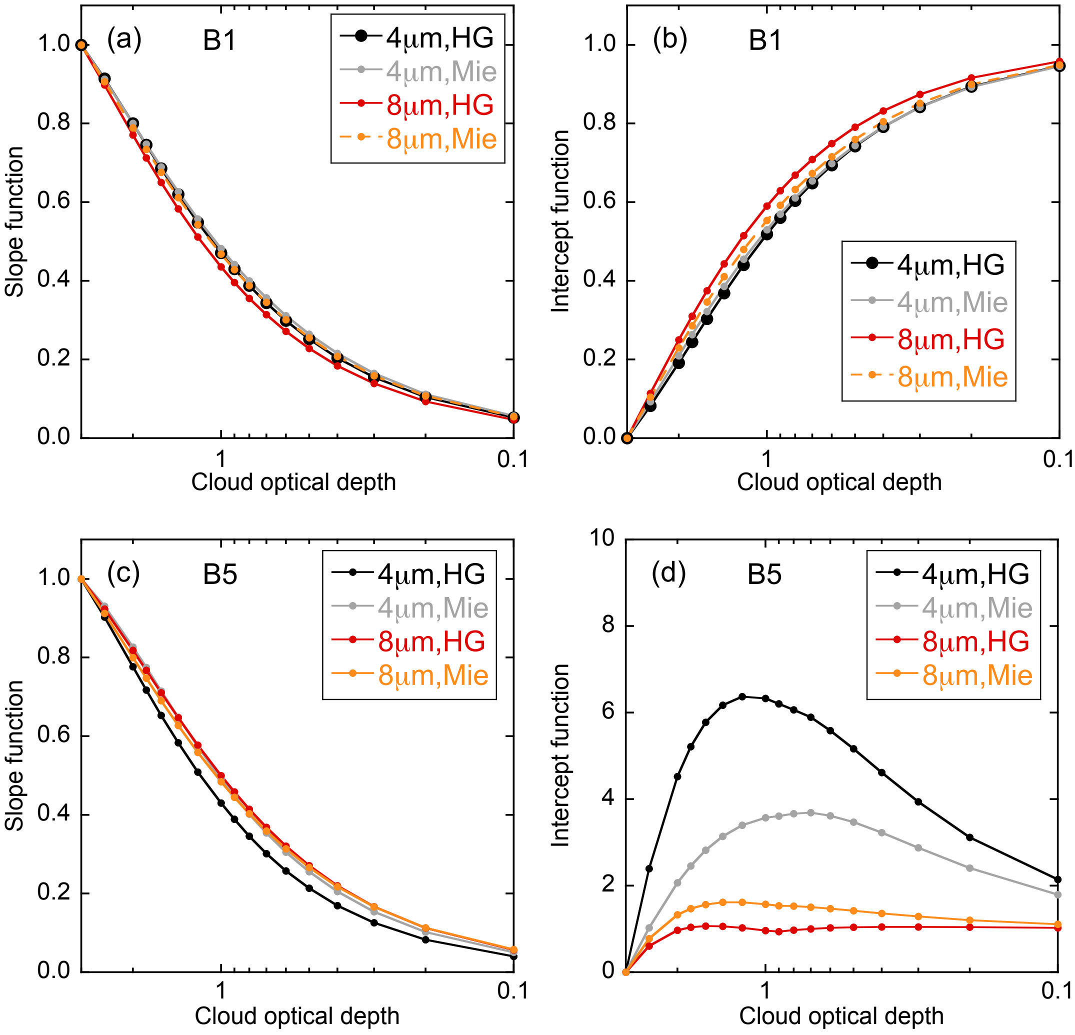

Figure 7. (a) Slope and (b) intercept functions derived from band B1 (400–870 nm wavelengths). (c) and (d) are the same as (a) and (b), but derived from band B5 (2110–2220 nm wavelengths). Each plot shows results for two cloud drop sizes (4 and 8 μm) and two types of phase functions (Henyey-Greenstein and Mie).

Preliminary Results for 3D effects

In this section we use Monte Carlo simulations to investigate how 3D effects modulate the spectrally-invariant relationship. We assume a cloud that is 2.5 km long and 0.4 km deep, as illustrated in Fig. A1(a). Cloud optical depths ranges between 3 and 0 in the east-west direction, while they are homogeneous in the south-north and vertical directions. Two illumination cases are included here: one is the sun is in the east; the other is the sun is in the west. Radiances from the former case are shown in Fig. A1(b).

3D effects on the spectrally-invariant behavior depend on sun-cloud-geometry and the sharpness of cloud edges for both band B1 (Fig. A2) and B5 (not shown). When the sun is in the east, simulated radiance from 3D calculations is similar to that from 1D calculations. Accordingly, the slope and intercept of the spectrally-invariant relationships are not sensitive to 1D or 3D calculations when the transition zone of interest is on the illumination side.

On the contrary, when the sun is in the west, radiance increases significantly at cloud optical depth of 3, because the west side of the cloud has a sharper edge and scatters more photons into the radiometer (Fig. A3(a)). The 3D effects on simulated radiance become less notable in the region toward the east. The significant increase in radiance for cloud optical depth of 3 causes a larger cloudy-to-clear ratio in the horizontal axis in Fig. A3(b), while the insignificant change for the rest of regions produces similar ratios in the vertical axis. As a result, all points shift to the right in Fig. A3(b). In addition, at cloud optical depth of 3, the huge increase in radiance is on the same magnitude for various wavelengths. For the fully clear region, however, the radiance at 440 nm is larger than that at 870 nm (as shown in Fig. A1(b)). These two factors cause that the shift to the right in Fig. A3(b) is more pronounced at 870 nm than that at 440 nm, which leads to a change in the linear relationship.

In summary, when the transition zone of interest is on the illuminated side, 3D effects have negligible impact on the spectrally-invariant behavior. When the transition zone of interest is on the shadowing side and the illuminated side has a sharper cloud edge, 3D effects could significantly change the linear relationship. Note that in the latter case, the cloud optical depth changes from 3 to 0 in a 50 m distance, which might be rare in reality. More cases are needed in order to better quantify the 3D effects on the spectrally-invariant behavior.

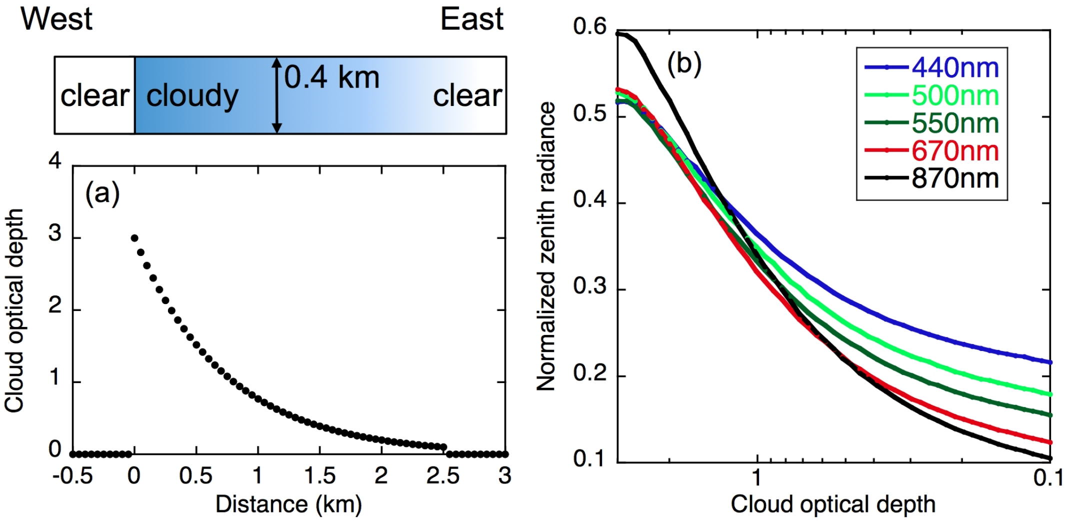

Figure A1. (a) A schematic illustration of a 2.5 km long and 0.4 km deep cloud with optical depth changing from 3 to 0. (b) Normalized zenith radiance simulated from 3D calculations. Cloud droplet size is 4 µm with a Mie phase function. Aerosol optical depth and spectral surface albedo are the same as the control run in Fig. 1. Solar zenith angle is 45 degree, while illumination is from the east and perpendicular to the plane of cloud inhomogeneity.

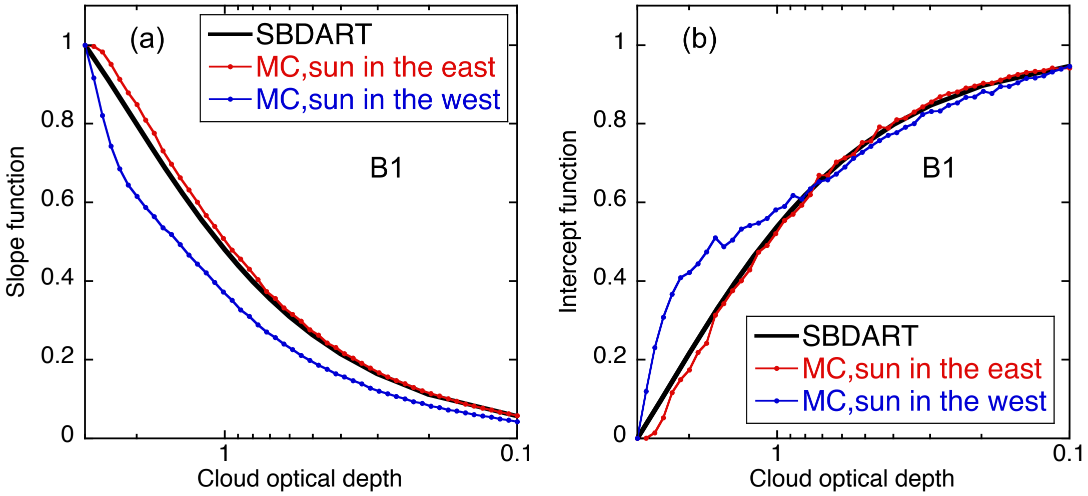

Figure A2. (a) Slope and (b) intercept functions derived from band B1 (400–870 nm wavelengths), using SBDART and Monte Carlo (MC) simulations. For MC simulations, we used two illumination cases: one is the sun is in the east; the other is the sun is in the west.

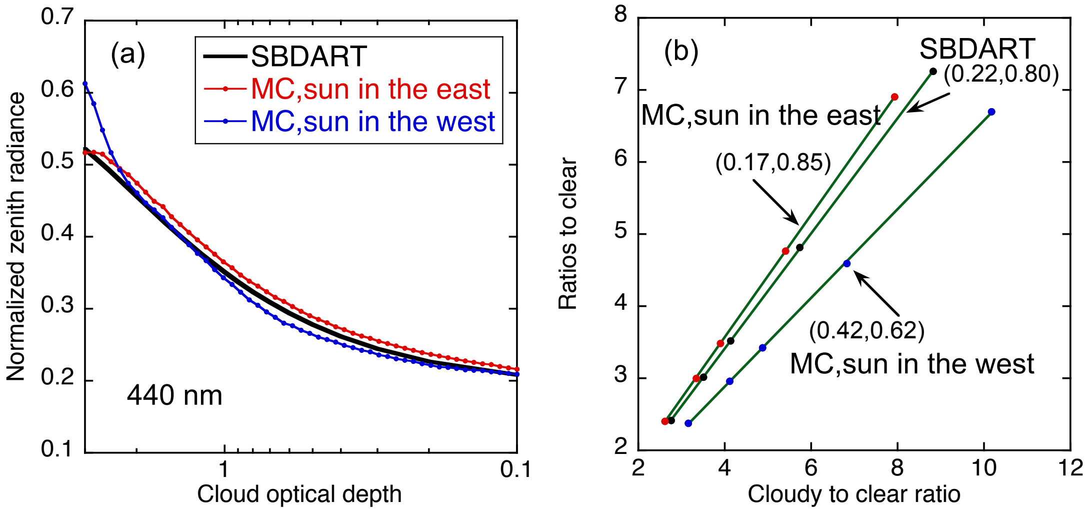

Figure A3. (a) Radiances at 440 nm simulated from SBDART and a Monte Carlo (MC) model. (b) Spectrally-invariant linear relationships at $\tau_c = 2.0$ for band B1 (400–870 nm) with a cloud drop effective radius values of 4 μm. Numbers in parentheses are the slope and intercept of the linear regression relationships (green lines).

Revised Paragraph

In this sensitivity test, we assume that cloud optical depth decreases from 3 to 0.1 between locations 100–250 m, as illustrated in Fig. 9a. Points at distance less than 100 m are fully cloudy with τ_c=3, points at distance greater than 250 m are fully clear (i.e., τ_c=0). As we expected, simulations (Fig. 9b) show that the slope function for the cloud at 5 km is more gradual than that for the cloud at 1 km. If we define the distance d^* such that

$$a\left(d^*\right) = e^{-1}, \tag{6}$$

where a is the slope of the spectrally-invariant relationship, we find the resulting d^* values are 172 m and 164 m for the cloud at 5 km and 1 km, respectively. This small difference in d^* suggests that a finite FOV has a negligible impact on spectrally-invariant behavior in the transition zone.